Cu-WO_3 Nanocomposite Prepared Through Solid-State Reaction Route: Characterization and Moisture Sensing Studies

Sanchita Singh[a,*], Narendra Kumar Pandey[a], and Priya Gupta[b]

[a] Sensors and Materials Research Laboratory, Department of Physics, University of Lucknow, Lucknow-226007, Uttar Pradesh, India

[b] Electronics and Communication Engineering Department, Integral University, Lucknow, U.P.-226026, India

*Corresponding Author Email: s.sanchita24@gmail.com

ABSTRACT

This paper reports characterization and moisture sensing properties of Cu-WO_3 nanocomposite prepared through solid-state reaction route. The crystallite size decreased from 72.4 nm to 55.3 nm when WO_3 was doped with 10 wt% Cu. The grain size of Cu doped WO_3 measured from Scanning electron microscopy (SEM) was decreased from 239 nm to 157 nm compared to pure WO_3. When pellet samples were exposed to humidity in the range 10 to 99% RH, the sensitivity of samples increased with an increase in annealing temperature**.** Cu doped WO_3 showed a highly enhanced value of sensitivity compared to pure WO_3. The Cu doped WO_3 sample annealed at 600°C showed best sensitivity of 18.62 MΩ/%RH. The hysteresis for pure and Cu doped WO_3 samples was within ±2.0% for 600°C annealing temperature. The problem of ageing was reduced, and response and recovery times improved when Cu was doped in WO_3.

Keywords: Sensor, composite, porosity, characterization

1. INTRODUCTION

The state of the art industry and general comforts in human life both need efficient monitoring of surrounding moisture level. This necessity has kept researchers and academicians equally dedicated for long to create novel materials having delightful sensitivity over various range of relative humidity (RH), good reproducibility and low hysteresis. These sensors must also withstand exposure to environmental pollutants. Porous stable metal oxides with reasonable mechanical toughness, grain boundary walls prove to be suitable materials for such applications [1]. The optimum quality and reasonable cost factors keep resistive humidity sensors ahead of capacitance, field-effect transistor and fiber-optic sensors [2]. These sensing elements with nano-grains and nano-porous structures offer high surface exposure for the adsorption of water molecules. For enhancing sensing parameters of semiconductors doping and/or mixing techniques are used to manipulate their properties [3]. V. Jeseentharani et al. investigated the moisture sensing properties of the composites of a 1:1 mole ratio of CuO-NiO, CuO-ZnO, and NiO-ZnO compound. CuO-NiO compound gives the maximum sensitivity and its response and recovery times were 80 s and 650 s, respectively [4]. Yawale et al. doped SnO_2 and ZnO with TiO_2 and Al_2O_3. They developed films of these materials through screen printing and measured the direct current resistance of the films with change of humidity [5]. Yadav et al. measured the direct current resistance with a change in humidity for annealing temperatures 200˚ C and 400˚ C and showed that the lanthanum oxide reflected the highest sensitivity out of pellets of niobium pentaoxide, neodymium oxide, and lanthanum oxide [6]. Stankova et al. studied the influence of annealing and operating temperatures on the gas-sensing properties of RF sputtered thin-film sensors [7]. Bittencourt et al. studied the characterization and gas sensing properties of WO_3:Ag films [8]. Zhou et al. synthesized highly ordered mesoporous tungsten oxide via the hard

template method [9]. Liu et al. synthesized tungsten oxide nanorods assembled microspheres by a facile hydrothermal process [10].

2. EXPERIMENTAL DETAILS

The chemical powders used for sample preparation were WO_3 (Loba Chemie, purity 99.99%) and Cu (Loba Chemie, purity 99.99%). 10 wt% of Cu along with 5 wt% polyvinyl alcohol (PVA) was added to WO_3 which acts as binder. This mixture was grinded to uniformity for 3 hours. Subsequently the powder was pressed into a pellet shape at ambient temperature under pressure of 250 MPa in a hydraulic press machine (M.B. Instruments, Delhi, India). The disc shaped fabricated pellet sample was having a diameter of 12 mm and thickness 2 mm. The pure WO_3 sample was fabricated in the similar manner by adding 5% PVA in WO_3 powder. The fabricated pellets were annealed in air at temperatures 300°C to 600°C for 3 hours in an electric muffle furnace (Ambassador, India).

The samples were exposed to moisture in a chamber. The schematic diagram of the chamber is shown in Fig.7. The calibration in the chamber was done with the help of a thermometer (±1°C) and a digital hygrometer (±1% RH). A multifunctional digital multi-meter (±0.001 MΩ, model VC-9818) was used to record variation in resistance with a change in relative humidity in the humidity range of 10-99% RH. Inside the chamber, the K_2SO_4 powder was used as humidifier and KOH pellets were used as dehumidifier.

3. CHARACTERIZATION

3.1. X-Ray Diffraction Analysis

X-ray diffraction was studied using XPERT PRO-Analytical XRD system (Netherland). It uses CuKα radiation source of wavelength 1.5406Å. Fig. 1 (a) and (b) shows X-ray patterns

for pure and Cu doped WO_3 annealed at 600°C respectively. The average crystallite size of the samples was calculated using Debye Scherer's formula given by equation (1):

$$D=0.9\,\lambda/\beta\,\cos\theta \quad (1)$$

where, D is the crystallite size (nm), λ is the X-ray wavelength (nm), θ is the Bragg angle (radians) and β is the full width at half maximum of the peak (radians).

The crystallite size calculated from Scherer's formula for pure WO_3 and Cu doped WO_3 sample annealed at 600°C was 72.4 nm and 55.3 nm respectively. While a majority of peaks at [(001) (110) (200) (331) (201) (212) (421) (203)] shifted to higher values of 2θ on the addition of Cu in WO_3, few peaks at [(101) (111) (102) (221)] shifted to slightly lower values of 2θ. Peaks at [(310) (400) (401)] maintained their earlier positions. Few additional peaks (perhaps of Cu) at [(211) (002) (220) (112) (222) (402)] appeared in XRD on the addition of Cu in WO_3

The presence of secondary Cu^{2+} phase in the sample confirmed the limit of substitutional incorporation of Cu^{2+} ions into WO_3 rather than interstitial incorporation. The broadening of the peaks indicates that the particles formed are in the range of nanometer [11]. The crystallite size decreased when Cu was doped. This might be due to the lattice strain induced in the doped WO_3 caused by the small mismatch of ionic radii between the host W^{6+} and dopant Cu^{2+}. The shifting of XRD peaks and a corresponding decrease of crystallite size suggest that Cu^{2+} ions were successfully incorporated into the WO_3 without altering the overall crystal structure[12].

3.2. Scanning Electron Micrograph

The surface morphology of the sensing element was studied using a scanning electron microscope unit (SEM, Leo-0430, Cambridge). SEM micrograph revealed that as the

temperature increased the porosity of the material increased forming clusters in Cu doped WO_3. The SEM micrograph of 600°C annealed Cu doped WO_3 showed that the sample was characterized by a typical porous structure without inside pores but many inter grain pores. Besides, the inter-granular pores were linked through the large pores [13]. The pore structures should be regarded as interconnected voids that formed a kind of capillary tubes. This structure favored the adsorption and condensation of water vapor. The grain size calculated from the SEM micrograph of pure and Cu doped WO_3 was 239 nm and 157 nm respectively. Fig. 2 (a) and (b) depicts micrographs of pure and Cu doped WO_3.

4. RESULT AND DISCUSSION

4.1. Humidification and Dehumidification Graphs

Fig. 3 (a) and (b) shows the variation in resistance with the change in relative humidity in the range 10%RH to 99%RH recorded for pure and Cu doped WO_3 samples annealed at temperatures 300°C-600°C respectively. An incessant decrease in the value of resistance with an increase in the %RH for pure WO_3 and Cu doped WO_3 samples annealed at temperatures 300-600°C was observed. Initially there is a sharp decline in the value of resistance when relative humidity is in the range 10 %RH-50 %RH while in high relative humidity range between 50 %RH-99 %RH, resistance decreases slowly. The Sensitivity of pure WO_3 was 17.42 MΩ/% RH in the 10-50% RH range and decreases to 4.67 MΩ/%RH in the 50-99% RH range. The sensitivity of Cu doped WO_3 was 38.12 MΩ/%RH in the 10-50% RH range and decreases to 2.71MΩ/%RH in the 50-99% RH range. This is because, at the low humidity conditions electrons might be trapped by the surface defects and released when the water molecules were co-adsorbed onto the surface causing some of the oxygen ions to be desorbed, and relatively high

resistance at low humidity was maintained. At high humidity conditions (>50%RH) the electrons might be trapped by the surface defects such as ionized oxygen vacancies and that these might be released when water molecules were adsorbed onto the defect sites, and therefore resulting in the reduction of the value of resistance at high humidity[14]. The sensitivity of the humidity sensor was defined as the change in resistance (ΔR) of sensing element per unit change in relative humidity (ΔRH %). The formula for calculation of the sensitivity of the sensing elements may be written as given below:

$$\text{Sensitivity} = (\Delta R) / (\Delta \%RH) \quad (2)$$

4.2. Hysteresis Graph

Fig. 5 (a) and (b) shows the hysteresis graph for pure and Cu doped WO_3 respectively for annealing temperature 600°C. The phenomenon of hysteresis might be understood in the manner that due to the adsorption of water on the surface of the sensing elements a chemisorbed layer was formed. The chemisorbed layer could be thermally desorbed only. Hence in the decreasing cycle of %RH, the initially adsorbed water was not removed fully leading to hysteresis. The value of hysteresis for both pure and doped samples was within ±2.0% for annealing temperature 600°C.

4.3. Ageing Effect

The sensing properties of pure and Cu doped WO_3 samples annealed at 600˚C were examined again in the humidity control chamber after six months and variation of resistance with %RH was recorded (Fig. 6 (a) and (b)). The sensitivity of pure WO_3 was reduced from 10.40 MΩ%RH to 8.87 MΩ%RH after six months whereas for Cu doped WO_3, sensitivity is reduced

from 18.62 MΩ%RH to18.47 MΩ%RH. It is observed that the ageing problem reduced when Cu was doped in WO_3 (Table 2).

Ageing effect in humidity sensors may be due either to prolonged exposure of the sensor surface to high humidity, adsorption of contaminants on the cation sites, loss of surface cations due to vaporization, solubility, and diffusion, or annealing to a less reactive structure, migration of cations away from the surface due to thermal diffusion[15]. Generally, the more sensitive a material is to humidity, the more it tends to be susceptible to ageing. Data were found to be generally reproducible over different operation cycles.

4.4. Response and Recovery Times

The response and recovery times are defined as the time taken to reach 90% of the total variation during humidification and dehumidification respectively. The response and recover times for pure WO_3 sample annealed at 600°C were 65 seconds and 105 seconds, respectively whereas the response and recovery times for the sample of Cu doped WO_3 annealed at 600˚C were 57 seconds and 99 seconds, respectively. The response and recovery times improved when WO_3 was doped with Cu as compared to pure WO_3. The response and recovery time also improved when annealing temperature was raised.

5. CONCLUSIONS

The crystallite size decreased from 72.4 nm to 55.3 nm when Cu was doped in WO_3 as compared to pure WO_3. The insignificant appearance of Cu peaks in XRD indicated that Cu made atomic substitution rather than interstitial substitution. The grain size of pure and Cu doped WO_3 was 239 nm and 157 nm respectively. When pellet samples are exposed to humidity, its sensitivity increased with an increase in annealing temperature for pure and Cu doped WO_3**.** The

Cu doped WO_3 sample annealed at 600°C showed best sensitivity of 18.62 MΩ/%RH. The hysteresis for sensing elements of Cu doped WO_3 was within ±2% for annealing temperature 600°C, much below market acceptable limit of ±5%. The problem of aging was reduced, and the response and recovery times improved when Cu was doped in WO_3. Cu doped WO_3 proved to be a robust, low cost, high strength sensor that gave low hysteresis, high reproducibility, and improved response and recovery times.

Acknowledgements: The authors would like to thanks The Birbal Sahni Institute of Paleobotany, Lucknow for the SEM facility and Department of Physics, University of Lucknow, Lucknow for the XRD facility.

REFERENCES

[1] Kulwicki, B. M., J. Amer. Ceram. Soc., vol. 74, pp. 697–708, 1991.

[2] Traversa, E., Sens. Act. B, pp. 135–156, 1995.

[3] Shimizu,Y., Arai, H., and Seiyama, T., Sens. Act., vol. 7, pp. 11–22, 1985.

[4] Jeseentharani, V., Jeyaraj, B., Pragasam, J., Dayalan, A., and Nagaraja, K. S., Sens. Trans. J., vol. 113, no. 2, pp. 48–55, Feb, 2010.

[5] Yawale, S. P., Yawale, S. S., and Lamdhade, G. T., Sens. Act. A, vol. 135, pp. 388–393, 2007.

[6] Yadav, B. C. and Singh, M., IEEE Sensors J., vol. 10, no. 11, pp. 1759–66, Nov, 2010.

[7] Stankova, M., Vilanova, X., Llobet, E., Calderer, J., Bittencourt, C., Pireaux, J. J., and Correig ,X., Sens. Act.B,vol.105,pp.271–277,2005.

[8] Bittencourt, C., Felicissimo, M. P., Felten, A., Nunes, L. A. O., Ivanov, P., Llobet, E., Pireaux, J. J.,andHoussiau,L.,Appl.Surf.Sci.,vol.250,pp.21–28,2005

[9] Zhou, Liang , Ren, Qijun , Zhou, Xufeng , Tang, Jiawei , Chen, Zhanghai, Yu, Chengzhong, Microporous andMesoporousMaterials,109pp.248–257,2008.

[10] Liu, Zhifu, Miyauchi, Masashio, Yamazaki, Toshinari, Shen, Yanbai, Sensors and Actuators B, 140.pp.514–519,2009.

[11] Zhuo, M., Chen, Y., Suna, J., Zhang, H., Guo, D., Zhang, H., Sens. Actuators B, Vol.186, pp.78-83, 2013.

[12] Toloman, D., Popa, A., Stan, M., Socaci, C., Biris, A., Katona, G., Appl. Surf. Sci., vol. 402, pp. 410-417, 2017.

[13] Parthibavarman, M., Hariharan, V., Sekar, C., Mater. Sci. Eng., Vol.31, Issue.5, pp.840- 844, 2011.

[14] Zhang, D., Zong, X., Li, P., Wu, Z., Zhang, Y., Sens & Act. B Chemical, Vol.226, pp. 52- 62, 2018.

[15] Gaury, J., Kelder, E. M., Bychkov, E. and Biskos, G., Thin Solid Films, 534, pp. 32–39, 2013

Table 2 Sensitivity of pure and Cu doped WO_3 samples

	Sensitivity (MΩ/%RH)					
Temp.	**Pure WO_3**			**Cu doped WO_3**		
	x	**y**	**z**	**X**	**y**	**z**
300°C	7.64	7.52	6.85	7.97	7.92	7.94
400°C	8.84	8.76	7.75	10.60	10.49	9.87
500°C	9.53	9.52	9.98	13.93	13.37	13.70
600°C	10.40	10.43	8.87	18.62	18.64	18.47

Where x is increasing cycle of relative humidity, y is decreasing cycle of relative humidity

And z is increasing cycle after six months

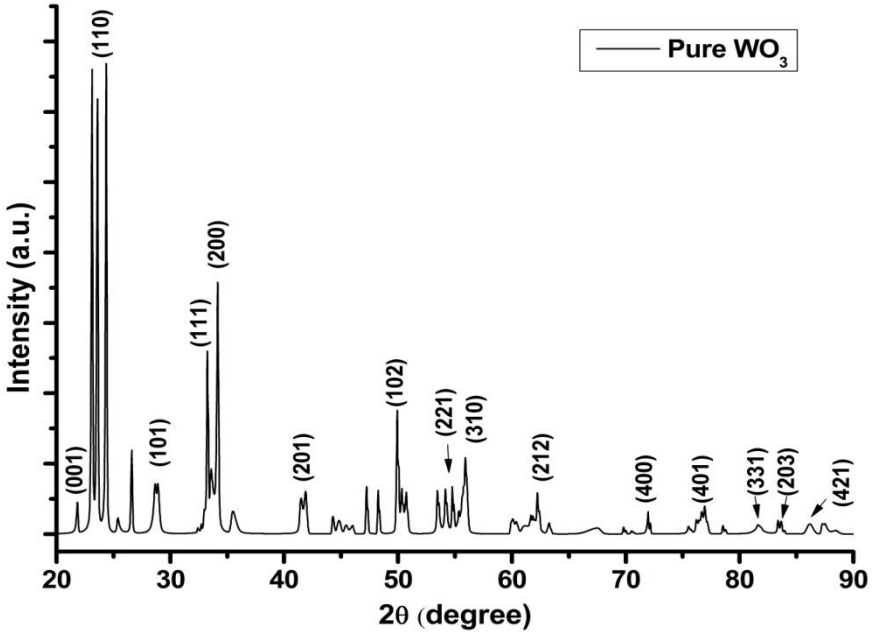

(a)

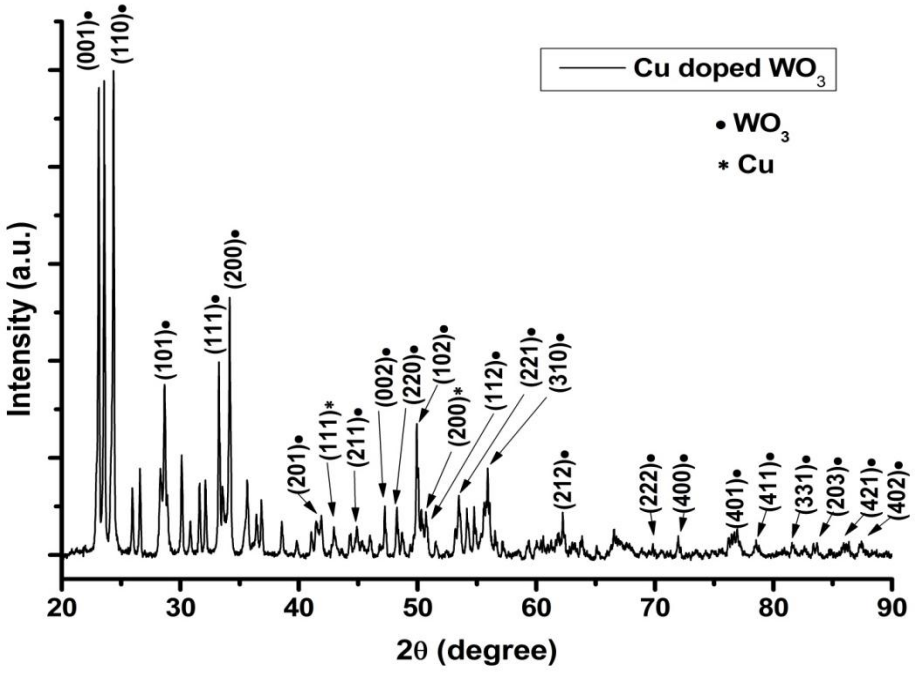

(b)

Fig. 1 XRD Pattern of (a) Pure WO_3 and (b) Cu doped WO_3 annealed at 600°C

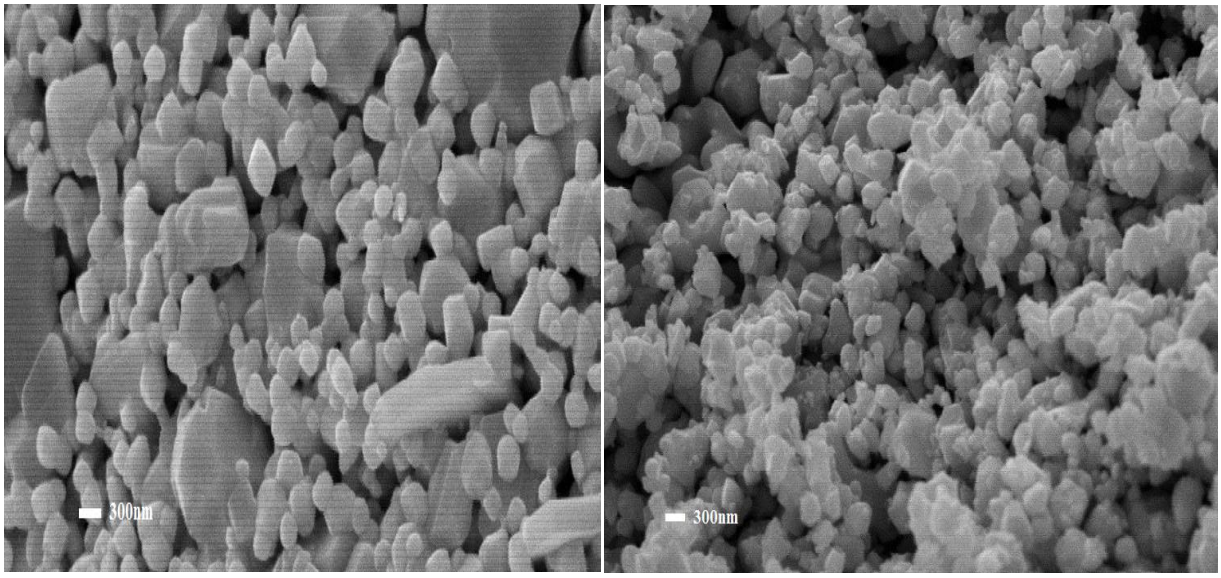

(a) (b)

Fig. 2 SEM micrograph of (a) pure WO_3 and (b) Cu Doped WO_3 annealed at 600°C

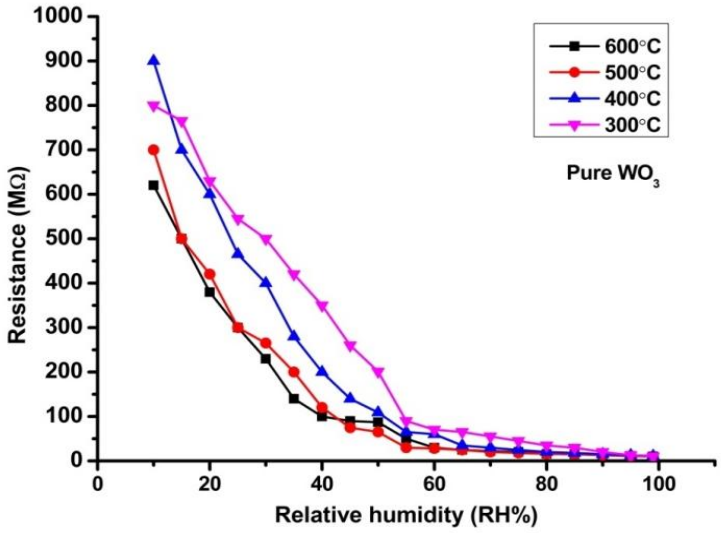

(a)

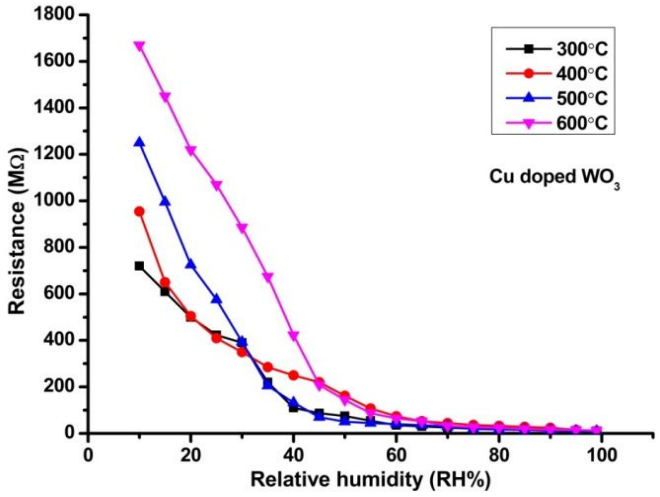

(b)

Fig. 3 Variation of resistance with relative humidity for (a) Pure WO_3 and (b) Cu Doped WO_3

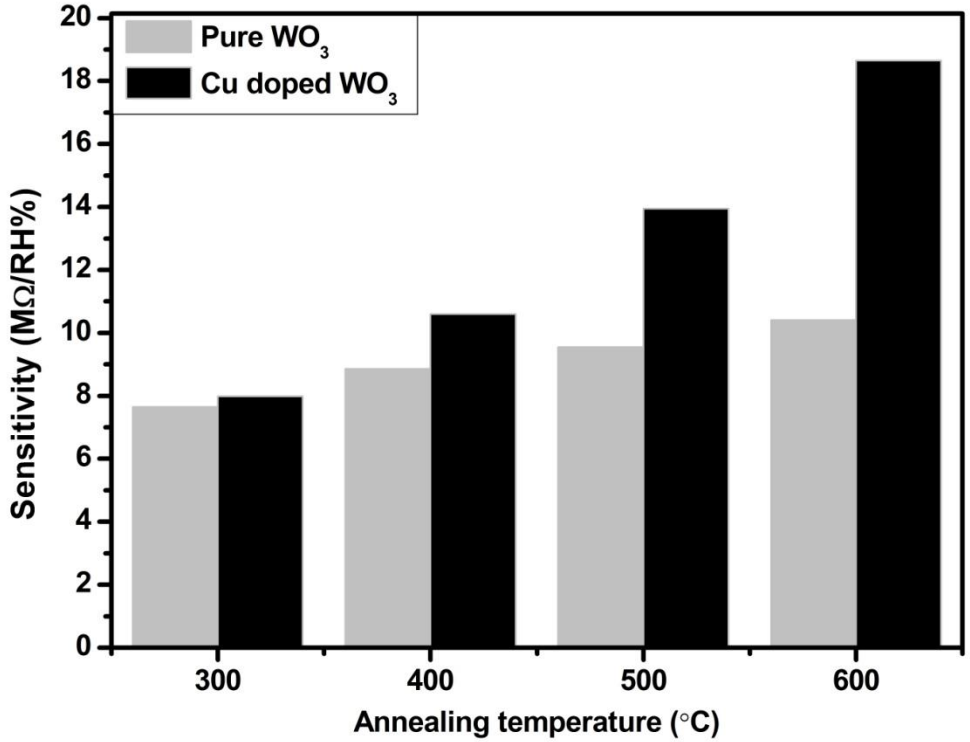

Fig. 4 Sensitivity vs Annealing Temperature Graph for Pure WO_3 and Cu Doped WO_3

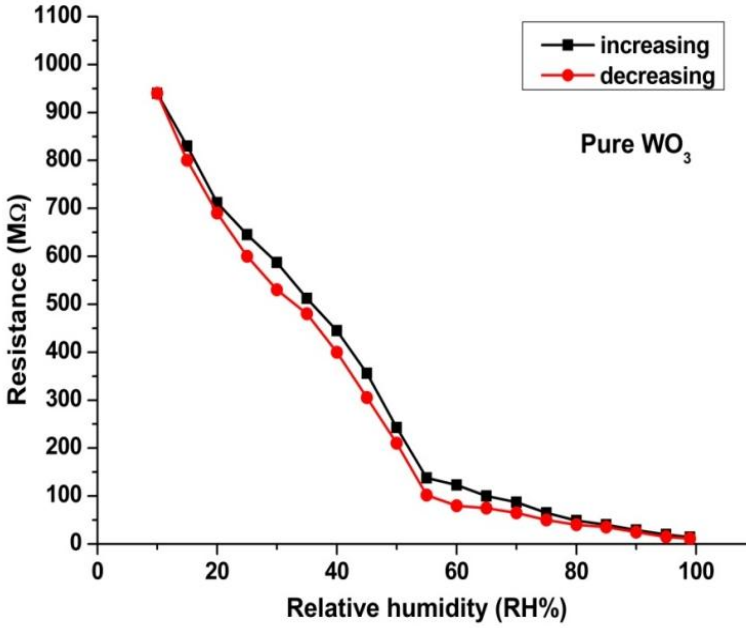

(a)

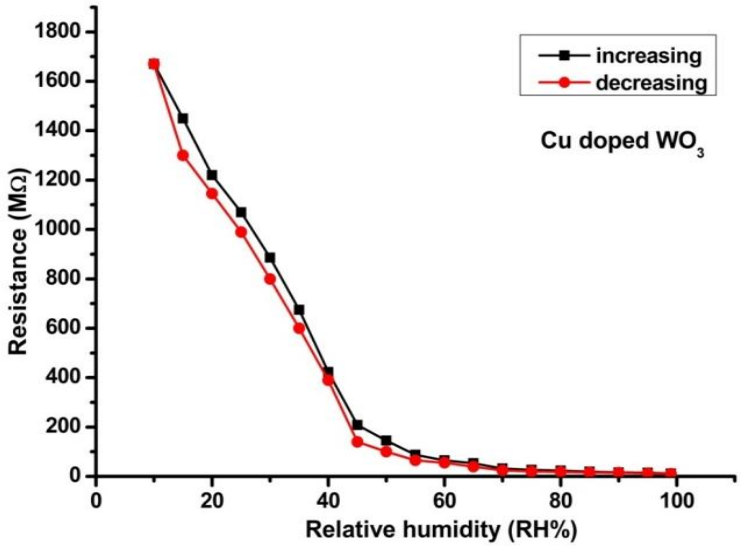

(b)

Fig. 5 Hysteresis Graph for (a) Pure WO_3 and (b) Cu Doped WO_3 at annealing temperature 600°C

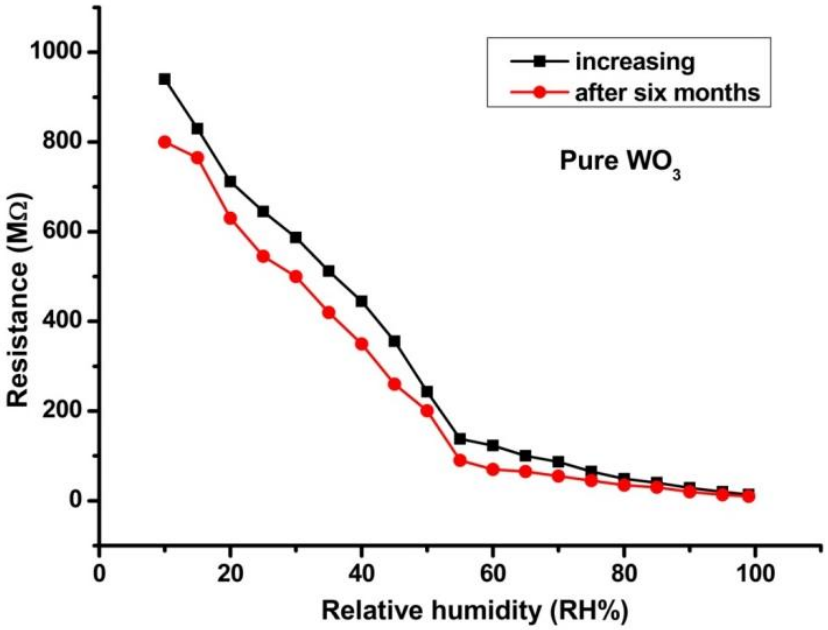

(a)

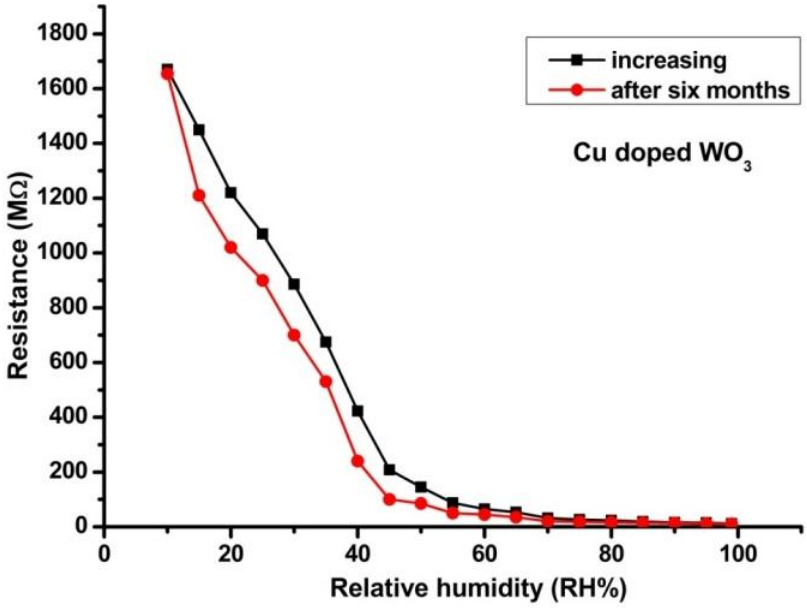

(b)

Fig. 6 Ageing Graph for (a) Pure WO_3 and (b) Cu Doped WO_3 annealed at 600˚C

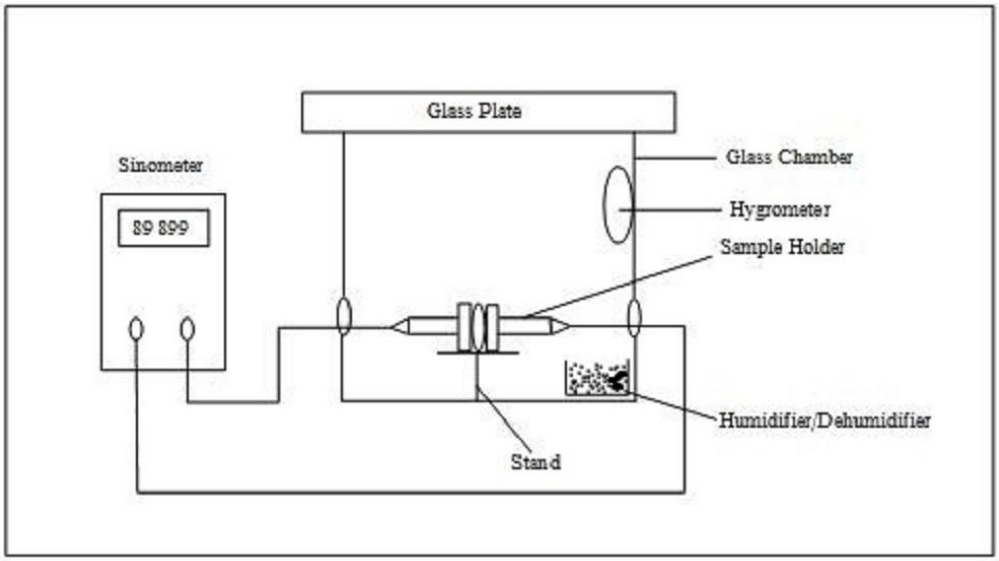

Fig. 7 Schematic Experimental Setup